# Two Contributions to the Theory of Annihilation of Positrons in Metals. I. Determination of the True Fermi Surface

CHANCHAL K. MAJUMDAR*
*Carnegie Institute of Technology, Pittsburgh, Pennsylvania*
(Received 12 May 1965)

The theory of positron annihilation in metals, including electron-positron and electron-electron interaction, is discussed. It is well known that the Coulomb force of the positron causes very major changes in the motion of the electrons. Nevertheless, it is established that a sharp "break" in the angular-correlation curve of the two $\gamma$ rays resulting from the singlet-state annihilation occurs at precisely those angles where it should be expected in the absence of electron-positron interaction. The break is an image of the discontinuity in the momentum distribution present in "normal" metals. Positron annihilation in metals is therefore a useful tool for the investigation of the true Fermi surface. It is also demonstrated that the slope of the angular-correlation curve at the Fermi momentum is related to the Gaussian curvature of the Fermi surface.

## INTRODUCTION

THE usefulness of positron annihilation in metals for the analysis of their various electronic properties has been recognized for quite some time. The two principal experimentally measured quantities are annihilation lifetime and angular-correlation of the emanating $\gamma$ rays resulting from the annihilation. In many cases, the effect of magnetic field on the annihilation process has also been investigated; in a few cases, the effect of temperature and pressure on the lifetime and angular-correlation curve has been reported. The earlier experimental work has been reviewed and discussed by Wallace.[1]

The lifetime measurements are done by standard delayed-coincidence technique. The annihilation rate in metals is about 1.1 to 2.2 times higher than that in free positronium ($2.00\times10^9$ sec$^{-1}$). It varies smoothly from high- to low-density metals and is lower in the latter. We shall, however, be mostly concerned with the interpretation of the angular-correlation experiments. These are done by the usual coincidence techniques with scintillation spectrometers. The intensity of the angular-correlation curve is a direct measure of a component of the center-of-mass momentum of the annihilating pair of particles. Extensive investigation along these lines is due to de Benedetti[2] and his group and Stewart[3] and his collaborators. These experiments are simple and direct, and the momentum distribution can be measured even for small impure samples of liquid metals. In fact, the precision available now enables Stewart[3] to integrate or differentiate his data numerically and to find the slope of the angular-correlation curve directly or to determine the complete momentum distribution of electrons in metals, which, in many cases, looks like the simple distribution predicted by the Sommerfeld theory of metals.

The effect of temperature on the angular-correlation curve has occasionally been studied systematically. Preliminary results in this direction were reported by Stewart *et al.*[3,4] For rare earths, the angular-correlation curve at several isolated temperatures has been obtained by Gustafson and McKintosh[5]; this has also been done for solid and liquid mercury.[6] In the second part of the work, we shall describe how the effective mass of the positron in metals can be determined from these experiments when systematically carried out.[4,7]

Theoretical studies on the annihilation of positrons in metals naturally started with an application of the free-electron theory of Sommerfeld to explain the lifetimes. This met with total failure. The total decay probability is directly proportional to the average density of electrons,

$$n=(\tfrac{4}{3}\pi a_0^3 r_s^3)^{-1},$$

($a_0$ is the Bohr radius), and thus proportional to $r_s^{-3}$. The experimental results indicate a much slower variation. R. Ferrell[8] attempted to correct the discrepancy by taking into account the Coulomb interaction between the electron and the positron. Since the bare Coulomb interaction is too strong to be correctly treated by the perturbation theory, he used the short-range potential derived by Bohm and Pines[9] in the plasma theory of the electron gas and was able to improve the theoretical result considerably. More ambitious attempts to take into account the interaction have been made by Kahana,[10] who used the Bethe-Goldstone equation[11] to incorporate the strong two-body correlation and secured very good agreement. Allowing for dynamic effects rather than using the

* Supported in part by National Science Foundation.
[1] P. R. Wallace, Solid State Phys. **10**, 1 (1960).
[2] G. Lang and S. de Benedetti, Phys. Rev. **108**, 914 (1957), and other papers.
[3] A. T. Stewart, Can. J. Phys. **35**, 168 (1957); A. T. Stewart, J. H. Kusmiss and R. H. March, Phys. Rev. **132**, 495 (1963), and other papers.
[4] A. T. Stewart and J. B. Shand, Bull. Am. Phys. Soc. **10**, 21 (1965).
[5] D. R. Gustafson and A. R. McKintosh, J. Phys. Chem. Solids **25**, 389 (1964).
[6] D. R. Gustafson, A. R. McKintosh, and D. J. Zaffarano, Phys. Rev. **130**, 1455 (1963).
[7] C. K. Majumdar, following paper, Phys. Rev. **140**, A237 (1965).
[8] R. A. Ferrell, Rev. Mod. Phys. **28**, 308 (1956).
[9] D. Bohn and D. Pines, Phys. Rev. **92**, 609 (1953).
[10] S. Kahana, Phys. Rev. **117**, 123 (1960); **129**, 1622 (1963).
[11] H. Bethe and J. Goldstone, Proc. Roy. Soc. **A238**, 551 (1957).

purely static interaction, the agreement has been made even better by Bergersen.[12]

In sheer contrast to the positron lifetimes, the angular-correlation curve seems to follow the behavior predicted by the free-electron theory extremely well.[3] The Fermi momentum of metals can be determined with an accuracy of 1.0% or better in favorable circumstances and agrees well with the free-electron value. By studying single crystals, the anisotropy of the Fermi surface in metals like Be and Li (due to the periodic lattice potential) has also been observed.[13] The sharp break at the Fermi momentum observed at low temperatures disappears when the metals are heated up; this will be discussed in paper II.[7]

In view of the fact that the positron lifetime measurements can be explained only by including strong electron-positron interaction,[10] the above results are surprising. It is the purpose of the work to show that there is a break in the angular-correlation curve at the Fermi momentum even if the interaction is considered. Different physical quantities are affected in quite different ways by the interaction. The result will be proved to all orders of the perturbation theory in electron-positron interaction for "normal" metals.

As usual, the term "normal" implies that the properties of such metals can be described by the perturbation theory and that a sharp Fermi surface, as defined by such an approach, exists in them. The concept of the true Fermi surface in the presence of electron-electron interaction has been clarified recently by the work of Kohn, Luttinger, and Ward[14] and is briefly discussed below. Our result remains true for the fully interacting electron gas in the presence of a periodic lattice potential.

It is also shown that the slope of the angular-correlation curve at the Fermi momentum is proportional to the square root of the reciprocal of the Gaussian curvature of the Fermi surface. This may be useful in the determination of the detailed shapes of the Fermi surfaces of metals.

## I. EVALUATION OF THE QUARTIC FORMULA OF ANNIHILATION

The theoretical work is based on current many-body techniques extended to the electron-positron system. The graphs arising in the perturbation theory need not be explicitly evaluated; the result follows from their structural properties. As said above, in the angular-correlation experiments one measures the probability that the $\gamma$ rays carry off a definite momentum $K_z$ along the vertical $z$ axis. We therefore want to know the probability $P(\mathbf{K})$ that the annihilating electron-positron pair has total momentum $\mathbf{K}$. Then by integrating over the $x$ and $y$ components of momentum we get the probability $P(K_z)$ for the $z$ component of momentum to be $K_z$ for the pair, which is experimentally measured. It is well known that $P(\mathbf{K})$ is given by the quartic formula[8,15]

$$P(\mathbf{K})=\lambda\langle\Psi_0|\sum_{\substack{\mathbf{p},\mathbf{p}'\\ \sigma,\sigma'}}\sigma\sigma' b^\dagger{}_{\mathbf{p},\sigma} \times d^\dagger{}_{\mathbf{K}-\mathbf{p},-\sigma} d_{\mathbf{K}-\mathbf{p}',-\sigma'} b_{\mathbf{p}',\sigma'}|\Psi_0\rangle, \quad (1.1)$$

where $\lambda=\alpha^2/16\pi^3m^2$, $\alpha$ is the fine-structure constant, and $m$ the electron mass. Here $b_{\mathbf{k},\sigma}$, $b^\dagger{}_{\mathbf{k},\sigma}$ are the annihilation and creation operators for electrons of momentum $\mathbf{k}$ and spin $\sigma$. Similarly, $d_{\mathbf{k},\sigma}$, $d^\dagger{}_{\mathbf{k},\sigma}$ are the corresponding operators for the positron. $\sigma=+1$ or $-1$ corresponds to spin up or down, respectively, along some fixed quantization axis. The expectation value is taken in the ground state of the fully interacting system, $\Psi_0$.

As a limiting case, consider a free-electron gas and a positron without interaction. The ground state is the filled Fermi sphere $\Phi_F$ for the electrons, and the positron in the zero-momentum state

$$\Psi_0=\Phi_F d^\dagger{}_{0,\sigma}|0\rangle,$$

where $|0\rangle$ denotes the vacuum state of the positron, and $\sigma=\pm1$. Then, clearly,

$$P(\mathbf{K})=\lambda\langle\Phi_F|b^\dagger{}_{\mathbf{K},-s}b_{\mathbf{K},-s}|\Phi_F\rangle =\lambda\langle\bar{n}_{\mathbf{K},-s}\rangle_F=\lambda\begin{cases}0, & K>k_F^-\\ 1, & K\leqslant k_F^-;\end{cases} \quad (1.2)$$

$k_F^-$ is the Fermi momentum of the electrons. So the probability that the $\gamma$-ray pair has the $z$ component of momentum $K_z$ is

$$P(K_z)=\int dK_x dK_y P(\mathbf{K}) =\lambda\pi[(k_F^-)^2-K_z^2]. \quad (1.3)$$

This is the usual parabolic formula for the free-electron gas.[8]

Going back to (1.1), we notice that we can put $\sigma'=\sigma$, since all the interactions we are going to consider are spin-independent.

$$P(\mathbf{K})=\lambda\langle\Psi_0|\sum_{\substack{\mathbf{p},\mathbf{p}'\\ \sigma}} b^\dagger{}_{\mathbf{p},\sigma}d^\dagger{}_{\mathbf{K}-\mathbf{p},-\sigma}d_{\mathbf{K}-\mathbf{p}',-\sigma}b_{\mathbf{p}',\sigma}|\Psi_0\rangle. \quad (1.4)$$

The fully interacting ground state is, of course, not known, and we have to use the perturbation theory to evaluate (1.4). The consistent approach here is through finite-temperature statistical mechanics, such as that described by Bloch and de Dominicis,[16] or Luttinger and Ward.[14]

There are several limiting processes involved, and a discussion, if not a proof in a mathematical sense, is clearly called for. The experimentally observed coinci-

[12] B. Bergersen, thesis, submitted to Brandeis University, 1964 (unpublished).

[13] A. T. Stewart, J. B. Shand, J. J. Donaghy, and J. H. Kusmiss, Phys. Rev. **128**, 118 (1962); J. J. Donaghy and A. T. Stewart, Bull. Am. Phys. Soc. **9**, 238 (1964).

[14] W. Kohn and J. M. Luttinger, Phys. Rev. **118**, 41 (1960); J. M. Luttinger and J. C. Ward, *ibid.* **118**, 1417 (1960).

[15] J. M. Jauch and F. Rohrlich, *The Theory of Photons and Electrons* (Addison-Wesley Publishing Company, Inc., Reading, Massachusetts, 1959).

[16] C. Bloch and C. de Dominicis, Nucl. Phys. **7**, 459 (1958).

dences are directly proportional to the number of positrons $N_+$ injected into the system; it is known that the thermalized positrons do not diffuse out again. Application of statistical mechanics presupposes at least a macroscopic density of positrons; clearly to analyze the experimental data we need only a term proportional to the number of positrons; in other words, we are interested in the extreme low-density limit of positrons.

The complication of working at finite temperature arises from the Kohn-Luttinger prescription[14] of the double limit involved. We must let the volume of the system go to infinity first and then let the temperature approach zero. The effect of interactions on the shape of the Fermi surface, as defined in the elementary Sommerfeld theory of metals, is not correctly described by the standard zero-temperature perturbation theory due to Brueckner, Goldstone, and Hugenholtz.[17] We shall define the Fermi surface of the interacting system precisely in Sec. IV. Here we note that the zero-temperature theory can describe the interacting system correctly, if and only if there is a definite symmetry requirement that demands the perturbed Fermi surface to have the same shape as the unperturbed one. This would be the case, for instance, in a gas of fermions interacting via a spherically symmetric potential. On the other hand, if the interaction is nonspherical, there is no reason why the Fermi surface should remain spherical. In the case of electrons in a metal, the interaction (Coulomb force) is spherically symmetric, but the unperturbed Fermi surface has only the symmetry of the lattice. The interaction would tend to distort the Fermi surface. Starting from the finite temperature statistical mechanical formulation, Kohn and Luttinger found certain anomalous diagrams,[14] in which a particle and a hole have the same momentum label—a situation impossible at zero temperature. The contribution of such diagrams, by taking the volume $\Omega\to\infty$ limit first, and then $T\to 0$ limit, is singular (the $\Omega\to\infty$ limit ensures that one energy level actually coincides with the true chemical potential). Reversing the order of the limits, one would *a priori* exclude such diagrams and reach an absurd conclusion that the true Fermi surface always coincides with the unperturbed one, no matter what the interaction is.

We therefore start at finite temperature to allow for any possible shift of the Fermi surface, due to the electron-positron interaction. We shall find that the break in the angular correlation curve occurs at the original Fermi surface. In Sec. IV, we include electron-electron interaction and show that the break occurs at the "true" Fermi surface.

The correct limiting procedure to evaluate (1.4) means that we calculate

$$\lim_{T\to 0}\lim_{\Omega\to\infty}\lim_{N_+\to 0} P(\mathbf{K}). \tag{1.5}$$

Here $N_+\to 0$ implies that we look for a term proportional to the number of positrons, $N_+$. Freed from the restriction of spherical Fermi surfaces, we shall be able to generalize our results formally to cases where a periodic potential is present.

## II. DIAGRAM ANALYSIS

The complete Hamiltonian for the system is

$$H=H_0+V, \tag{2.1}$$

$$H_0=\sum_{\mathbf{k},\sigma}\epsilon_{\mathbf{k}}{}^{-}b^{\dagger}{}_{\mathbf{k},\sigma}b_{\mathbf{k},\sigma}+\sum_{\mathbf{k},\sigma}\epsilon_{\mathbf{k}}{}^{+}d^{\dagger}{}_{\mathbf{k},\sigma}d_{\mathbf{k},\sigma}. \tag{2.2}$$

The interaction $V$ will include either electron-positron interaction or electron-electron interaction or both, depending on the occasion. We shall consider the perturbation $V$ to all orders.

Let $\mu_-$ be the true chemical potential for the electrons and $\mu_+$ that for the positrons. Let $N_-$ and $N_+$ be the total number of electrons and positrons present, respectively. Then

$$P(\mathbf{K})=\lambda\sum_{\mathbf{p},\mathbf{p}',\sigma}\langle b^{\dagger}{}_{\mathbf{p},\sigma}b_{\mathbf{p}',\sigma}d^{\dagger}{}_{\mathbf{K}-\mathbf{p},-\sigma}d_{\mathbf{K}-\mathbf{p}',-\sigma}\rangle$$
$$=\lambda\sum_{\mathbf{p},\mathbf{p}',\sigma}G(\mathbf{p},\mathbf{p}';\mathbf{K};\sigma), \tag{2.3}$$

where $\langle\ \rangle$ denotes an average over a grand canonical ensemble. In the Heisenberg representation,

$$G(\mathbf{p},\mathbf{p}';\mathbf{K};\sigma)$$
$$=\frac{\mathrm{Tr}e^{-\beta(H-\mu_--N_--\mu_+N_+)}b^{\dagger}{}_{\mathbf{p},\sigma}b_{\mathbf{p}',\sigma}d^{\dagger}{}_{\mathbf{K}-\mathbf{p},-\sigma}d_{\mathbf{K}-\mathbf{p}',-\sigma}}{\mathrm{Tr}e^{-\beta(H-\mu_--N_--\mu_+N_+)}}. \tag{2.4}$$

Going over to the interaction representation in the usual way, we have

$$P(\mathbf{K})=\lambda\sum_{\mathbf{p},\mathbf{p}',\sigma}\frac{\langle T(F(\beta)b^{\dagger}{}_{\mathbf{p},\sigma}b_{\mathbf{p}',\sigma}d^{\dagger}{}_{\mathbf{K}-\mathbf{p},-\sigma}d_{\mathbf{K}-\mathbf{p}',-\sigma})\rangle}{\langle F(\beta)\rangle}$$
$$=\lambda\sum_{\mathbf{p},\mathbf{p}',\sigma}\langle T(F(\beta)b^{\dagger}{}_{\mathbf{p},\sigma}b_{\mathbf{p}',\sigma}d^{\dagger}{}_{\mathbf{K}-\mathbf{p},-\sigma}d_{\mathbf{K}-\mathbf{p}',-\sigma})\rangle_L, \tag{2.5}$$

where

$$F(\beta)=e^{\beta H_0}e^{-\beta H}. \tag{2.6}$$

$T$ denotes the usual time-ordering operator. The subscript $L$ denotes that the average is evaluated from linked diagrams alone. $F(\beta)$ has the well-known expansion

$$F(\beta)=\sum_{i=0}^{\infty}(-)^i\int_{\beta>u_1>u_2>\cdots>u_i>0}du_1du_2\cdots du_i$$
$$\times V(u_1)V(u_2)\cdots V(u_i), \tag{2.7}$$

with

$$V(u)=e^{uH_0}Ve^{-uH_0}. \tag{2.8}$$

Here we have made use of the fact that $V$ conserves the

[17] *The Many-Body Problem*, edited by C. DeWitt (John Wiley & Sons, Inc., New York, 1959).

number of particles. The diagram analysis of (2.7) is well known, and we simply write down the rules for drawing diagrams associated with (2.5). The quartic operator of (2.5), which contributes $\lambda$, is to be treated as a special vertex carrying total momentum $\mathbf{K}$; in analogy with a topological term in the theory of linear graphs, we shall refer to it as a "rooted" vertex. It will occur once in each diagram and will be denoted by a dashed line.

We first consider electron-positron interaction only.

$$V=\sum_{\substack{\mathbf{k}_1,\mathbf{k}_2\\ \sigma_1,\sigma_2}}\sum_{\substack{\mathbf{q}\\ q\neq 0}} V_q b^\dagger_{\mathbf{k}_1-\mathbf{q},\sigma_1} d^\dagger_{\mathbf{k}_2+\mathbf{q},\sigma_2} d_{\mathbf{k}_2,\sigma_2} b_{\mathbf{k}_1,\sigma_1}. \quad (2.9)$$

The restriction $q\neq 0$ comes from the fact that the smeared-out positive background exactly cancels the average attraction of the electrons, and the entire system is neutral with regard to the positrons on the average. The rules for diagrams are:

(i) Draw all possible $n$th-order linked diagrams; in each there will be $n$ interactions and only one rooted vertex. In the zeroth order, the rooted vertex alone occurs. With the $n$th-order diagram, associate a factor $(-)^{n+n_l}/n!$, where $n_l$ is the number of closed fermion loops.

(ii) For each electron line labeled by a single arrowhead and momentum $\mathbf{k}$, associate a factor

$$\beta^{-1}(\zeta_l-\epsilon_{\mathbf{k}}^-)^{-1}, \quad \zeta_l=(2l+1)\frac{\pi i}{\beta}+\mu_-, \quad (l=0,\pm 1,\cdots).$$

(iii) For each positron line labeled by a double arrowhead and momentum $\mathbf{k}$, write a factor

$$\beta^{-1}(\xi_m-\epsilon_{\mathbf{k}}^+)^{-1}, \quad \xi_m=(2m+1)\frac{\pi i}{\beta}+\mu_+, \quad (m=0,\pm 1,\cdots).$$

(iv) The electron line that begins and ends at the same time gives a factor

$$\beta^{-1}(e^{\zeta_l 0+})/(\zeta_l-\epsilon_{\mathbf{k}}^-);$$

similarly, the positron line under the same condition gives

$$\beta^{-1}(e^{\xi_m 0+})/(\xi_m-\epsilon_{\mathbf{k}}^+).$$

(v) At each vertex associate the proper $V$ factor with correct momentum transfer. Note that the electron-positron interaction is attractive and each $V$ has an implicit negative sign.

(vi) At each vertex the incoming $\zeta_l+\xi_m$ equals the outgoing $\zeta_{l'}+\xi_{m'}$. These restrictions give "energy" conserving $\delta$ functions multiplied by $\beta$. Hence count a factor $\beta$ for each such $\delta$ function.

(vii) Sum over all the $l$'s and $m$'s, and the free momentum indices. The spin summation requires a little consideration. This gives a factor $2^{n_l-1}$, where $n_l$ is the number of particle loops. The subtraction of 1 comes from the fact that the annihilation occurs in a definite singlet state; the spin of the electron may be up or down, but this fixes the positron spin. We shall see below that we have to consider only one positron loop. The other electron loops give a factor 2 each. The $l$ and $m$ sums can be carried out in the usual way.[14]

As examples, we write down the contribution of the zeroth- and first-order diagrams (Fig. 1): zeroth order [Fig. 1(a)]:

$$2\lambda\sum_{\mathbf{p}}\sum_{l,m}\frac{e^{\zeta_l 0+}}{\beta(\zeta_l-\epsilon_{\mathbf{p}}^-)}\frac{e^{\xi_m 0+}}{\beta(\xi_m-\epsilon^+_{\mathbf{K}-\mathbf{p}})}=2\lambda\sum_{\mathbf{p}} f^-(\epsilon_{\mathbf{p}}^-)g^-(\epsilon^+_{\mathbf{K}-\mathbf{p}}).$$

First order [Fig. 1(b)]:

$$-2\lambda\sum_{\mathbf{p},\mathbf{p}'}\sum_{\substack{l_1,l_2\\ m_1,m_2}} V_{|\mathbf{p}-\mathbf{p}'|}\frac{\beta\delta(\xi_{m_1}+\zeta_{l_1},\xi_{m_2}+\zeta_{l_2})}{\beta(\zeta_{l_1}-\epsilon_{\mathbf{p}}^-)\beta(\zeta_{l_2}-\epsilon_{\mathbf{p}'}^-)\beta(\xi_{m_1}-\epsilon_{\mathbf{K}-\mathbf{p}}^+)\beta(\xi_{m_2}-\epsilon_{\mathbf{K}-\mathbf{p}'}^+)}=4\lambda\sum_{\mathbf{p},\mathbf{p}'} V_{|\mathbf{p}-\mathbf{p}'|}\frac{f^-(\epsilon_{\mathbf{p}}^-)f^+(\epsilon_{\mathbf{p}'}^-)g^-(\epsilon_{\mathbf{K}-\mathbf{p}}^+)g^+(\epsilon_{\mathbf{K}-\mathbf{p}'}^+)}{\epsilon_{\mathbf{p}}^-+\epsilon^+_{\mathbf{K}-\mathbf{p}}-\epsilon^-_{\mathbf{p}'}-\epsilon^+_{\mathbf{K}-\mathbf{p}'}}.$$

$f^-$ and $g^-$ denote the Fermi functions for the electron and the positron, respectively, $f^+=1-f^-$, $g^+=1-g^-$, as usual, and $\delta(m,n)$ is used for $\delta_{mn}$ where the argument is complicated.

## III. EFFECTS OF ELECTRON-POSITRON INTERACTION

Since the number of positrons is vanishingly small, the effect of the chemical potential $\mu_-$ of the electrons will be negligible. This is, of course, true even in the presence of electron-electron interaction, which causes a finite shift of the electronic chemical potential. Drawing a self-energy graph of an electron interacting with a positron (Fig. 2), we notice that the summation over $\mathbf{k}$, the momentum of the positron hole, goes essentially over the Fermi sphere of the positron, and we have a quantity like

$$\sum_{\mathbf{k}} F(\mathbf{k})g^-(\epsilon_{\mathbf{k}}^+),$$

where $F$ involves the matrix elements of the potential and other momentum sums. In view of the fact that the number of positrons is extremely small, we can replace $F(\mathbf{k})$ by its value at $\mathbf{k}=0$ and carry out the summation over the positron Fermi function $g^-(\epsilon_{\mathbf{k}}^+)$, which

gives just the number of positrons $N_+$.

$$\lim_{N_+\to 0}\sum_{\mathbf{k}} F(\mathbf{k})g^-(\epsilon_{\mathbf{k}}^+)=F(0)\sum_{\mathbf{k}} g^-(\epsilon_{\mathbf{k}}^+)=F(0)N_+. \quad (3.1)$$

In the limit $N_+\to 0$ this becomes negligible, so that $\mu_-$ is unaffected to $0(N_+)$.

All quantities in higher powers of $N_+$ will, of course, be negligible. In evaluating (1.5) we are looking for a quantity just proportional to $N_+$. This implies that all the diagrams we should consider will be "ladder-like" with regard to the positrons; in other words, there should be only one hole line for the positron when we draw graphs for evaluating (1.5). Otherwise, from each additional hole line present in the diagram, we will get a factor $N_+$ by the above arguments.

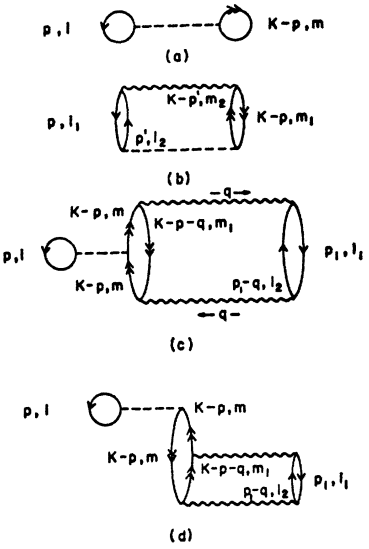


FIG. 1. Some diagrams arising in the perturbation theory; dashed line—the rooted vertex of the quartic operator; single arrow—electron; double arrow—positron; wavy line—interaction.

Let us recall that the quartic operator for annihilation gives a "rooted" vertex denoted by a dashed line in the graphs. We shall call the rooted vertex "symmetrical," if the electron and the positron, both in particle states, scatter both into particle states or both into hole states. The vertex is also symmetrical if they were both initially in hole states (Fig. 3). Otherwise the rooted vertex is "unsymmetrical" (Fig. 4). We do not have to consider scattering of positron holes into positron holes in the limit $N_+\to 0$. One can now verify the following: the contribution from all diagrams in which the rooted vertex is symmetrical and does not have a vertex correction can be written in the form

$$P_s(\mathbf{K})=\sum_{\mathbf{p}} f^-(\epsilon^-_{\mathbf{K}-\mathbf{p}})g^-(\epsilon_{\mathbf{p}}^+)F(\mathbf{p},\mathbf{K}). \quad (3.2)$$

The proof is simple. Consider time-ordered diagrams. At the symmetric vertex, the two incoming particles have total momentum $\mathbf{K}$. For the conditions stated above there are one electron and one positron hole present in the diagram with total momentum $\mathbf{K}$, since momentum is conserved at every vertex. If the incoming

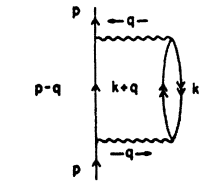


FIG. 2. Self-energy graph of an electron propagator due to positrons.

particles scatter into holes, the rooted vertex occurs at the upper end of the diagram, and the statement is obviously true. Similarly, if the rooted vertex is at the lower end of the diagram, the statement is true and is more tautology. If the particles scatter into particles, the same holds, because for a ground-state diagram the sum of the momenta at any horizontal section for particles and holes, with proper signs, must be zero, and for this subset of graphs only one electron hole is present at the instant of the rooted vertex. From these electron and positron holes, we get the factors $f^-(\epsilon^-_{\mathbf{K}-\mathbf{p}})$ and $g^-(\epsilon^+_{\mathbf{p}})$, the simple Fermi functions.

In the limit of zero temperature, this will give a break in the angular correlation curve at the Fermi momentum. For,

$$\lim_{T\to 0}\lim_{\Omega\to\infty}\lim_{N_+\to 0} P_s(\mathbf{K})=\lim_{T\to 0}\lim_{\Omega\to\infty} f^-(\epsilon_{\mathbf{K}}^-)F_T(\mathbf{K})\sum_{\mathbf{p}} g^-(\epsilon_{\mathbf{p}}^+)$$

$$=\lim_{T\to 0} f^-(\epsilon_{\mathbf{K}}^-)F_T(\mathbf{K})N_+=\theta^-(\epsilon_{\mathbf{K}}^-)F_0(\mathbf{K})N_+, \quad (3.3)$$

where $\theta^-(\epsilon_{\mathbf{K}}^-)$ is a step function which is 1 if $\epsilon_{\mathbf{K}}^-\leqslant\mu_-$, and zero otherwise. As examples, we draw a few of these graphs (Fig. 5). The simplest topological class in this category is that of the ladders.

Let us now consider a few diagrams that do not give such a free factor $f^-(\epsilon_{\mathbf{K}}^-)$ and therefore are unlikely to have any contribution that will give a "break" at zero temperature. They may be called "unsymmetrical" graphs as the rooted vertex is unsymmetrical (Fig. 6). Two topological classes may be easily characterized; they are electron-hole positron scattering and those with a vertex correction. The latter is used in the usual sense. All these diagrams occur in second or higher orders of the perturbation theory. Those with vertex correction

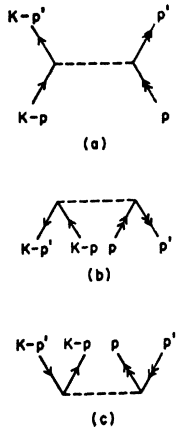


FIG. 3. Symmetrical rooted vertex.

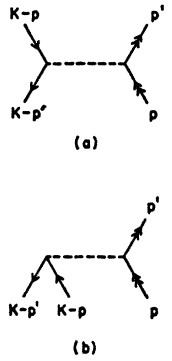


FIG. 4. Unsymmetrical rooted vertex.

show infrared divergence for long-range forces that can be cured in standard fashion. These unsymmetrical graphs will give rise to a "tail" in the angular correlation curve.

In the limit of zero temperature, the angular correlation curve is no longer a simple parabola with a sharp cutoff at the Fermi momentum. However, it remains a curve with a discontinuity in slope at the Fermi momentum.

## IV. ELECTRON-ELECTRON INTERACTION

Formal inclusion of electron-electron interaction is simple, if it can be treated by the perturbation theory. The result within this framework is almost obvious: The angular correlation curve still shows a break at the Fermi momentum, and the experiment shows up the true Fermi surface of the fully interacting system of electrons. This will follow from the fact that the diagrams we considered above are just a subset of the set of all diagrams that contribute to (1.5).

Rules for drawing diagrams can easily be extended to include electron-electron interaction. The complete Hamiltonian for the system is

$$\begin{aligned}\bar{H}=&\sum_{\mathbf{k},\sigma}(\epsilon_{\mathbf{k}}^{-}-\mu_{-})b^{\dagger}_{\mathbf{k},\sigma}b_{\mathbf{k},\sigma}+\sum_{\mathbf{k},\sigma}(\epsilon_{\mathbf{k}}^{+}-\mu_{+})d^{\dagger}_{\mathbf{k},\sigma}d_{\mathbf{k},\sigma}\\&+\tfrac{1}{2}\sum_{\substack{\mathbf{k}_1,\mathbf{k}_2\\ \sigma_1,\sigma_2}}\sum_{\substack{\mathbf{q}\\ q\neq 0}}\bar{V}_q b^{\dagger}_{\mathbf{k}_1+\mathbf{q},\sigma_1}b^{\dagger}_{\mathbf{k}_2-\mathbf{q},\sigma_2}b_{\mathbf{k}_2,\sigma_2}b_{\mathbf{k}_1,\sigma_1}\\&+\sum_{\substack{\mathbf{k}_1,\mathbf{k}_2\\ \sigma_1,\sigma_2}}\sum_{\substack{\mathbf{q}\\ q\neq 0}}V_q b^{\dagger}_{\mathbf{k}_1+\mathbf{q},\sigma_1}d^{\dagger}_{\mathbf{k}_2-\mathbf{q},\sigma_2}d_{\mathbf{k}_2,\sigma_2}b_{\mathbf{k}_1,\sigma_1}. \quad (4.1)\end{aligned}$$

$q=0$ terms are always cancelled by the background of uniform positive charge. Note, however, that the electronic interaction has a factor $\frac{1}{2}$ and is repulsive.

Let us first consider the diagrams that give the break, that is, the graphs with a symmetric vertex without any vertex correction. The electron-electron interaction can do one of the following things. First it can embellish the subset with self-energy parts on each electron line in arbitrary fashion; in this case, the subset will serve as the "skeleton" diagrams, and we propose to call these the "skeleton set." Secondly, it can generate new topological classes; for example, a vertex correction at the rooted vertex on the electron lines. In the former case,

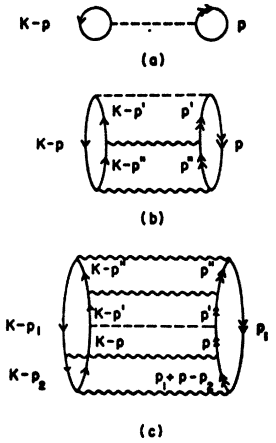


FIG. 5. Some symmetrical graphs that give the "break" at the Fermi momentum.

the break is shown to persist, but now at the true Fermi surface.

Let us consider the "skeleton set" and start with the simplest diagram. We can put arbitrary self-energy parts on the electron line in Fig. 1(a). It is clear that for the extremely low-density limit of positrons we get lines in the diagram carrying momentum $\mathbf{K}$, and one expects the break due to the Fermi functions from these lines (Fig. 7). However, there are anomalous diagrams present and the chemical potential is not equal to $\epsilon_F^{-}$, the unperturbed Fermi energy.

Consider the simplest of such diagrams [Fig. 7(b)]. The diagram is anomalous, because a hole and a particle carry the same momentum, which would not be possible in a zero-temperature graph. Its contribution is, neglecting sign and numerical factors,

$$\begin{aligned}&\lambda\sum_{\mathbf{p},\mathbf{p}'}\bar{V}_{|\mathbf{p}-\mathbf{p}'|}\beta\sum_{l_1}\frac{e^{\zeta l_1 0+}}{\beta(\zeta_{l_1}-\epsilon_{\mathbf{p}'}^{-})}\\&\qquad\times\sum_{m}\frac{e^{\xi m 0+}}{\beta(\xi_m-\epsilon^{+}_{\mathbf{K}-\mathbf{p}})}\sum_{l}\frac{1}{\beta^2(\zeta_l-\epsilon_{\mathbf{p}}^{-})^2}\\&=\lambda\sum_{\mathbf{p},\mathbf{p}'}V_{|\mathbf{p}-\mathbf{p}'|}f^{-}(\epsilon^{-}_{\mathbf{p}'})g^{-}(\epsilon^{+}_{\mathbf{K}-\mathbf{p}})\sum_{l}\frac{1}{\beta(\zeta_l-\epsilon^{-}_{\mathbf{p}})^2}. \quad (4.2)\end{aligned}$$

The $l$ sum must be carefully done. If we naïvely pass to the zero-temperature limit, we get zero;

$$\frac{1}{\beta}\sum_{l}\frac{1}{(\zeta_l-\epsilon_{\mathbf{p}}^{-})^2}\rightarrow\frac{1}{2\pi i}\oint\frac{d\zeta}{(\zeta-\epsilon_{\mathbf{p}}^{-})^2}=0. \quad (4.3)$$

The fact that such diagrams do not give vanishing contribution was first pointed out by Kohn and Luttinger,[14] and the correct evaluation is

$$\begin{aligned}\frac{1}{\beta}\sum_{l}\frac{1}{(\zeta_l-\epsilon_{\mathbf{p}}^{-})^2}&=\frac{1}{2\pi i}\int_{c}\frac{d\zeta f^{-}(\zeta)}{(\zeta-\epsilon_{\mathbf{p}}^{-})^2}\\&=-\left(\frac{\partial f^{-}}{\partial\zeta}\right)_{\zeta=\epsilon_{\mathbf{p}}^{-}}\xrightarrow[\beta\rightarrow\infty]{}\delta(\epsilon_{\mathbf{p}}^{-}-\mu_{-}), \quad (4.5)\end{aligned}$$

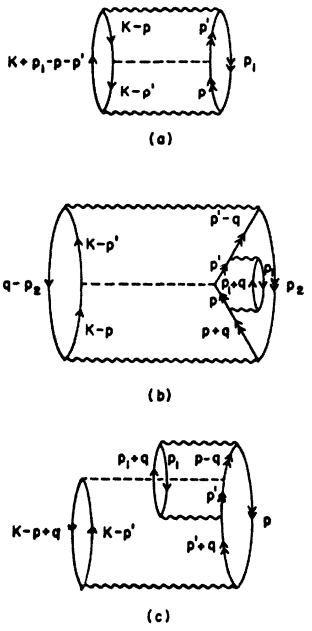


FIG. 6. Some unsymmetrical graphs.

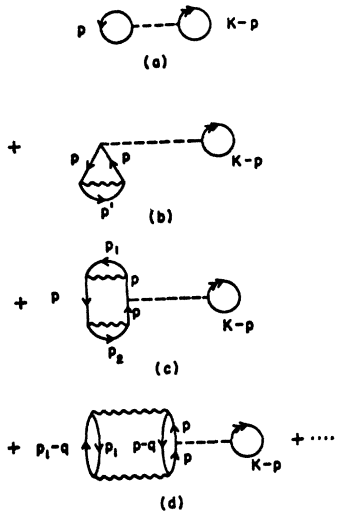


FIG. 7. Insertion of self-energy parts on the electron line (due to electron-electron interaction).

according to the procedure of Luttinger and Ward.[14] In the zero-temperature limit, the contribution is, in fact, singular. Such singular parts are responsible for the shift of the chemical potential from the unperturbed Fermi energy to the true value $\mu_-$. The situation is similar to the mass renormalization in field-theoretic problems.

With insertion of self-energy parts the electron propagators become renormalized. Since the interaction is translationally invariant, they are still diagonal in momentum space. Consider a graph in which an electron line enters, things of arbitrary complexity happen, and then a single-particle line emerges. The initial state and the final state must have the same character. Such modified propagators for momentum state $\mathbf{k}$ we shall call $S_{\mathbf{k}}'(\zeta_l)$. Let us denote by $\beta G_{\mathbf{k}}(\zeta_l)$ the contribution of all irreducible self-energy parts, that is, the diagrams that cannot be separated by cutting a single line. We have conveniently taken out a factor $\beta$ that comes from the over-all $l$ conservation. Then the modified propagator can be written as

$$\begin{aligned} S_{\mathbf{k}}'(\zeta_l)=&\beta^{-1}(\zeta_l-\epsilon_{\mathbf{k}}{}^-)^{-1}+\beta^{-1}(\zeta_l-\epsilon_{\mathbf{k}}{}^-)^{-1}\\ &\times G_{\mathbf{k}}(\zeta_l)(\zeta_l-\epsilon_{\mathbf{k}}{}^-)^{-1}+\beta^{-1}(\zeta_l-\epsilon_{\mathbf{k}}{}^-)^{-1}\\ &\times G_{\mathbf{k}}(\zeta_l)(\zeta_l-\epsilon_{\mathbf{k}}{}^-)^{-1}G_{\mathbf{k}}(\zeta_l)(\zeta_l-\epsilon_{\mathbf{k}}{}^-)^{-1}+\cdots\\ =&\beta^{-1}[\zeta_l-\epsilon_{\mathbf{k}}{}^--G_{\mathbf{k}}(\zeta_l)]^{-1}. \end{aligned} \tag{4.6}$$

With this definition we can write down the contribution of the diagrams of Fig. 7 as

$$C_1\simeq\lambda\sum_{\mathbf{p}}\sum_l\frac{e^{\zeta_l 0+}}{\beta(\zeta_l-\epsilon_{\mathbf{p}}{}^--G_{\mathbf{p}}(\zeta_l))}\sum_m\frac{e^{\xi_m 0+}}{\beta(\xi_m-\epsilon^+{}_{\mathbf{K}-\mathbf{p}})},$$

and, in the limit of low positron density,

$$C_1\simeq\lambda N_+\sum_l\frac{e^{\zeta_l 0+}}{\beta(\zeta_l-\epsilon_{\mathbf{K}}{}^--G_{\mathbf{K}}(\zeta_l))}. \tag{4.7}$$

The $l$ sum actually represents the mean occupation $\bar{n}_{\mathbf{K}}$ of the momentum state $\mathbf{K}$ for the interacting electron gas. A detailed discussion of this quantity has been given by Luttinger.[18] Since the definition of the true Fermi surface is based on this quantity, it will be convenient to summarize his results here. Let

$$\bar{n}_{\mathbf{K}}=\beta^{-1}\sum_l\frac{e^{\zeta_l 0+}}{\zeta_l-\epsilon_{\mathbf{K}}{}^--G_{\mathbf{K}}(\zeta_l)}. \tag{4.8}$$

In the limit of zero temperature, this function may have a discontinuity. In this limit,

$$\bar{n}_{\mathbf{K}}=(2\pi i)^{-1}\int_{\mu_--i\infty}^{\mu_-+i\infty}d\zeta(e^{\zeta 0+})/[\zeta-\epsilon_{\mathbf{K}}{}^--G_{\mathbf{K}}(\zeta)]. \tag{4.9}$$

In deforming the contour, the following analytic properties of $G_{\mathbf{K}}(\zeta)$ are useful: $G_{\mathbf{K}}(\zeta)$ is analytic everywhere except the real axis; also, for $x$ real,

$$G_{\mathbf{K}}(x\pm i0+)=K_{\mathbf{K}}(x)\mp iJ_{\mathbf{K}}(x),\quad K_{\mathbf{K}},\ J_{\mathbf{R}}\text{ real}, \tag{4.10}$$

so $G_{\mathbf{K}}$ has a discontinuity $J_{\mathbf{K}}$ across the real axis. Further

$$J_{\mathbf{K}}(x)\gtrless 0, \tag{4.11}$$

and as $x$ approaches $\mu_-$

$$J_{\mathbf{K}}(x)=C_{\mathbf{K}}(x-\mu_-)^2,\quad C_{\mathbf{K}}>0. \tag{4.12}$$

By closing the contour to the left, (4.9) becomes

$$\bar{n}_{\mathbf{K}}=(2\pi i)^{-1}\int_{-\infty}^{\mu_-}dx\{[x-\epsilon_{\mathbf{K}}{}^--K_{\mathbf{K}}(x)-iJ_{\mathbf{K}}(x)]^{-1}\text{c.c.}\}. \tag{4.13}$$

[18] J. M. Luttinger, Phys. Rev. **119**, 1153 (1960); **121**, 942 (1961).

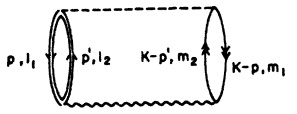


FIG. 8. A diagram of first order in electron-positron interaction, with electron propagator completely renormalized.

$K_{\mathbf{K}}$ and $J_{\mathbf{K}}$ are, in general, smooth functions of $\mathbf{K}$ and any possible discontinuity in $\bar{n}_{\mathbf{K}}$ as function of $\mathbf{K}$ can come only from a singularity in the integrand in the neighborhood of $\mu_-$ where $J_{\mathbf{K}}$ vanishes. Consider the $\mathbf{K}$ values which satisfy the equation

$$\mu_- - \epsilon_{\mathbf{K}}^- - K_{\mathbf{K}}(\mu_-) = 0. \tag{4.14}$$

This describes a surface in the $\mathbf{K}$ space. If there were no electron-electron interaction, $K_{\mathbf{K}}=0$ and (4.14) would define the Fermi surface in the conventional free-electron theory. Luttinger calls the surface defined by (4.14) the Fermi surface of the interacting system. Studying (4.14) in detail, he has shown, within the framework of the perturbation theory, that the momentum distribution of the electron system has a discontinuity on this Fermi surface.

The Fermi surface so defined has the same volume as the unperturbed one; the interactions may, at most, deform it. In the case of spherically symmetric interaction, where symmetry requires it to remain a sphere, its radius must remain $k_F^-$, the unperturbed Fermi momentum.

Returning to the positron problem, we shall consider the first-order diagram in electron-positron interaction, but take the electron propagators to be completely renormalized by the electron-electron interaction. Let us denote by $S_k^+(\xi_m)$, the positron propagator. Then the contribution of the above diagram (Fig. 8) can be written as

$$C_2 \simeq \lambda \sum_{\mathbf{p},\mathbf{p}'} V_{|\mathbf{p}-\mathbf{p}'|} \sum_{\substack{l_1,l_2\\ m_1,m_2}} S'_{\mathbf{p}}(\zeta_{l_1}) S'_{\mathbf{p}'}(\zeta_{l_2}) S^+_{\mathbf{K}-\mathbf{p}}(\xi_{m1}) S^+_{\mathbf{K}-\mathbf{p}'}(\xi_{m_2}) \beta\delta(\zeta_{l_1}+\xi_{m_1}, \zeta_{l_2}+\xi_{m_2}), \tag{4.15}$$

where $\delta(m,n)\equiv\delta_{mn}$, as before. It is convenient to utilize the fact that the renormalized propagator satisfies the integral representation[18,19]

$$S'_{\mathbf{p}}(\zeta_l) = \int_{-\infty}^{\infty} \frac{\rho_{\mathbf{p}}(\eta)}{\zeta_l - \eta} d\eta. \tag{4.16}$$

$\rho_{\mathbf{p}}(\eta)$ is the spectral function of the propagator; its analytic properties have been investigated in detail.[18] For a noninteracting system, $\rho_{\mathbf{p}}(\eta)=\delta(\eta-\epsilon_{\mathbf{p}}^-)$. So

$$C_2 \simeq \lambda \sum_{\mathbf{p},\mathbf{p}'} V_{|\mathbf{p}-\mathbf{p}'|} \sum_{\substack{l_1,l_2\\ m_1,m_2}} \int_{-\infty}^{\infty}\int_{-\infty}^{\infty} d\eta_1 d\eta_2 \frac{\rho_{\mathbf{p}}(\eta_1)\rho_{\mathbf{p}'}(\eta_2)\beta\delta(\zeta_{l_1}+\xi_{m_1}, \zeta_{l_2}+\xi_{m_2})}{\beta^4(\zeta_{l_1}-\eta_1)(\zeta_{l_2}-\eta_2)(\xi_{m_1}-\epsilon_{\mathbf{K}-\mathbf{p}}^+)(\xi_{m_2}-\epsilon_{\mathbf{K}-\mathbf{p}'}^+)}. \tag{4.17}$$

We perform the $l$, $m$ sums by the usual method, to obtain

$$C_2 \simeq 2\lambda \sum_{\mathbf{p},\mathbf{p}'} V_{|\mathbf{p}-\mathbf{p}'|} \int_{-\infty}^{\infty}\int_{-\infty}^{\infty} d\eta_1 d\eta_2 \frac{\rho_{\mathbf{p}}(\eta_1)\rho_{\mathbf{p}'}(\eta_2) f^-(\eta_1) f^+(\eta_2) g^-(\epsilon^+_{\mathbf{K}-\mathbf{p}}) g^+(\epsilon^+_{\mathbf{K}-\mathbf{p}'})}{\eta_1+\epsilon^+_{\mathbf{K}-\mathbf{p}}-\eta_2-\epsilon^+_{\mathbf{K}-\mathbf{p}'}}. \tag{4.18}$$

In the limit of low positron density, we get

$$C_2 \simeq 2\lambda N_+ \sum_{\mathbf{p}'} V_{|\mathbf{K}-\mathbf{p}'|} \int\int_{-\infty}^{\infty} d\eta_1 d\eta_2 \frac{\rho_{\mathbf{K}}(\eta_1)\rho_{\mathbf{p}'}(\eta_2) f^-(\eta_1) f^+(\eta_2) g^+(\epsilon^+_{\mathbf{K}-\mathbf{p}'})}{\eta_1-\eta_2-\epsilon^+_{\mathbf{K}-\mathbf{p}'}}$$

$$\simeq 2\lambda N_+ \int_{-\infty}^{\infty} d\eta_1 \rho_{\mathbf{K}}(\eta_1) f^-(\eta_1) F(\eta_1; \mathbf{K}, V). \tag{4.19}$$

$F(\eta_1; \mathbf{K}, V)$ is a smooth function of $\mathbf{K}$. Now the spectral function may be written as[19]

$$\rho_{\mathbf{K}}(\eta_1) = \delta(\eta_1 - \epsilon_{\mathbf{K}}^- - K_{\mathbf{K}}(\eta_1)) + \tilde{\rho}_{\mathbf{K}}(\eta_1), \tag{4.20}$$

where $\tilde{\rho}_{\mathbf{K}}(\eta_1)$ is smooth function, and the integral over $\tilde{\rho}_{\mathbf{K}}(\eta_1)$ gives nothing singular. Taking the $\delta$-function part alone, and using

$$\rho_{\mathbf{K}}(\eta_1) = z_{\mathbf{K}} \delta(\eta_1 - E_{\mathbf{K}}), \tag{4.21}$$

where

$$E_{\mathbf{K}} = \epsilon_{\mathbf{K}}^- + K_{\mathbf{K}}(E_{\mathbf{K}}) \tag{4.22}$$

is a true single-particle excitation energy of the system of the electrons, and

$$z_{\mathbf{K}}^{-1} = \{1 - [\partial K_{\mathbf{K}}(\xi)/\partial\xi]\}_{\xi=E_{\mathbf{K}}} \tag{4.23}$$

[19] P. Nozières and J. M. Luttinger, Phys. Rev. **127**, 1423, 1431 (1962).

is a measure of the discontinuity of the momentum distribution at the Fermi surface, one gets the contribution

$$C_2=2N_+z_{\mathbf{K}}\lambda f^-(E_{\mathbf{K}})F(E_{\mathbf{K}};\mathbf{K},V)+\cdots. \quad (4.24)$$

In the limit of zero temperature, this gives the "break" at the true Fermi surface.

Now it is easy to generalize the result to any arbitrary graph of the skeleton set. Obviously, the contribution of any such graph can be written as

$$\bar{C}\simeq\lambda\sum_{\mathbf{p}}g^-(\epsilon^+_{\mathbf{K}-\mathbf{p}})\int_{-\infty}^{\infty}d\eta_1\rho_{\mathbf{p}}(\eta_1)\times f^-(\eta_1)F(\eta_1;\mathbf{p},V,\bar{V}). \quad (4.25)$$

The function $F(\eta_1;\mathbf{p},V,\bar{V})$ is a smooth function. As before, in the limit of low positron density, the contribution has a part containing a Fermi function with the true single-particle excitation energy, $E_{\mathbf{K}}$;

$$\bar{C}\simeq\lambda N_+z_{\mathbf{K}}\int_{-\infty}^{\infty}\delta(\eta-E_{\mathbf{K}})f^-(\eta)F(\eta;\mathbf{K},V,\bar{V})d\eta+\cdots$$

$$\simeq\lambda N_+z_{\mathbf{K}}f^-(E_{\mathbf{K}})F(E_{\mathbf{K}};\mathbf{K},V,\bar{V})+\cdots. \quad (4.26)$$

This part gives the break at the true Fermi surface in the limit of zero temperature. The other parts from these diagrams give smoothly varying contributions and will therefore add to the tail of the angular-correlation curve. This completes the demonstration that the angular-correlation curve will show a kink at the true Fermi surface.

The generalization of this result to the case where the electrons and positrons move in an external periodic potential of a lattice is completely straightforward and will not be described here in detail. The above conclusion is based on the validity of the perturbation theory and is therefore restricted to normal metals. It is natural to inquire what happens in superconductors where the perturbation theory has failed. It is found, as one might expect, that there is no kink in the angular-correlation curve at the Fermi momentum; otherwise the curve is hardly affected. The entire change is of the order of the ratio of the energy gap to the Fermi energy, and detection of such a change necessarily demands extremely high precision not presently available.

## V. RELATION OF THE SLOPE OF THE ANGULAR-CORRELATION CURVE WITH THE GAUSSIAN CURVATURE OF THE FERMI SURFACE

Another interesting quantity that can be extracted out of the angular-correlation experiment is the Gaussian curvature[20] of the Fermi surface. We shall show that the slope of the correlation curve at the Fermi momentum is proportional to the square root of the reciprocal of the Gaussian curvature of the Fermi surface. Since the curve at zero temperature is continuous but not differentiable, one has to take the slope at $(k_F^-\pm0)$. At finite temperature, there is no difficulty.

We shall use the free electron model entirely in this section. According to Eq. (1.3), the probability $P(K_z)$ goes to zero at the Fermi momentum, but the approach to the Fermi momentum, which is reflected in the slope of $P(K_z)-K_z$ curve, will be determined by the curvature of the Fermi surface. Considering the spherical Fermi surface at zero temperature, we get

$$\left.\frac{dP(K_z)}{dK_z}\right|_{k_F^-}=-2\pi\lambda k_F^-. \quad (5.1)$$

Since the Gaussian curvature of a sphere of radius $a$ is $1/a^2$, its reciprocal $R$ is $a^2$,

$$\left.\frac{dP(K_z)}{dK_z}\right|_{k_F^-}=-2\pi\lambda R^{1/2}. \quad (5.2)$$

Let us consider the electron gas at finite temperature, but neglect any positron momentum for the present.

$$P(K_z)=\lambda\int_{-\infty}^{\infty}\int dK_xdK_y\times\left[\exp\left\{\frac{K_x^2+K_y^2+K_z^2-(k_F^-)^2}{2mk_BT}\right\}+1\right]^{-1}$$

$$=2\pi\lambda mk_BT\ln\left[1+\exp\left\{\frac{(k_F^-)^2-K_z^2}{2mk_BT}\right\}\right] \quad (5.3)$$

and

$$\frac{dP}{dK_z}=-2\pi\lambda K_z\Big/\left[\exp\left\{\frac{K_z^2-(k_F^-)^2}{2mk_BT}\right\}+1\right]. \quad (5.4)$$

Since the Fermi function is singular at zero temperature, the limit of zero temperature is nonuniform and has to be taken with care. For comparison with experimental results, we take the limit $T\to0$, with $K_z=k_F^--0$,

$$\lim_{T\to0,(K_z=k_F^--0)}[dP(K_z)/dK_z]=-2\pi\lambda k_F^-. \quad (5.5)$$

The right limit $(K_z=k_F^-+0)$ goes to zero:

$$\lim_{T\to0(K_z=k_F^-+0)}\frac{dP(K_z)}{dK_z}=0. \quad (5.6)$$

At finite temperature, there is no difficulty:

$$\left.\frac{dP(K_z)}{dK_z}\right|_{k_F^-,T}=-\tfrac{1}{2}\times2\pi\lambda k_F^-=-\lambda\pi k_F^-. \quad (5.7)$$

[20] B. Spain, *Tensor Calculus* (Oliver and Boyd, Edinburgh, 1953).

Hence the slope at finite temperature is half in magnitude of the value at zero temperature. The agreement of this result with the experimental curves of Stewart on sodium is excellent.[3]

Once again, we can write (5.7) as

$$\left.\frac{dP(K_z)}{dK_z}\right|_{k_F^-,T} = -\lambda\pi R^{1/2}. \tag{5.8}$$

The spherical Fermi surface is of course trivial, but the corresponding results can also be easily proved for a general ellipsoidal Fermi surface. One can also incorporate the effect of positron momentum easily.[7] For a spherical surface, the result is

$$\left.\frac{dP(K_z)}{dK_z}\right|_{k_F^-,T} = -\pi\lambda R^{1/2}\left[1-\frac{1}{\pi^{1/2}}\left(\frac{m_+^*T}{mT_F}\right)^{1/2}\right]. \tag{5.9}$$

$m_+^*$ is the positron effective mass; the measurement of this quantity will be considered in Part II of the work.

These results can be sharpened a little further by considering only a locally ellipsoidal Fermi surface. Suppose we can represent the energy surface in the neighborhood of the Fermi momentum $k_F^-$ by

$$E=\mu_- - a(k_F^- - K_z)+bK_x^2+cK_y^2, \tag{5.10}$$

where $K_z$ is along the *normal* to the Fermi surface at $k_F^-$. Hence the surface on which $E=\mu_-$ is given in the vicinity of $k_F^-$ by

$$-a(k_F^- - K_z)+bK_x^2+cK_y^2=0. \tag{5.11}$$

The area of the Fermi surface at $K_z$ is given by the area of the ellipse

$$bK_x^2+cK_y^2=-a(K_z-k_F^-)$$

and is equal to

$$\pi a(k_F^- - K_z)/(bc)^{1/2}. \tag{5.12}$$

The number of electrons at $K_z$ contributing to annihilation is

$$P(K_z)=\text{const}\int_{(K_z)} dK_x dK_y \theta^-(\epsilon_{\mathbf{K}}^-).$$

$\theta^-(\epsilon_{\mathbf{K}}^-)$ is the zero-temperature limit of the Fermi function; thus

$$P(K_z)=\text{const}\pi a(k_F^- - K_z)/(bc)^{1/2}. \tag{5.13}$$

Hence

$$\left.\frac{dP(K_z)}{dK_z}\right|_{k_F^-} = -\text{const}\frac{\pi a}{(bc)^{1/2}}. \tag{5.14}$$

To calculate the Gaussian curvature $R^{-1}$, we calculate the principal radii of curvature in the $xz$, $yz$ planes. For the $xz$ plane, $K_y=0$.

$$bK_x^2=-a(K_z-k_F^-).$$

$$\frac{1}{R_x(k_F^-)}=\left.\frac{d^2K_x/dK_z^2}{[1+(dK_x/dK_z)^2]^{3/2}}\right|_{k_F^-}=-\frac{2b}{a}. \tag{5.15}$$

Similarly,

$$[R_y(k_F^-)]^{-1}=-(2c/a). \tag{5.15'}$$

Now,

$$R=R_xR_y=4bc/a^2, \tag{5.16}$$

and so

$$\left.\frac{dP(K_z)}{dK_z}\right|_{k_F^-,T=0} = -\text{const}2\pi R^{1/2}. \tag{5.17}$$

At finite temperature one gets

$$\left.\frac{dP(K_z)}{dK_z}\right|_{k_F^-,T} = -\text{const}\pi R^{1/2}. \tag{5.18}$$

The factor $\frac{1}{2}$ comes from the Fermi function being equal to $\frac{1}{2}$ at finite temperatures exactly at the Fermi energy. This precise factor $\frac{1}{2}$ is a result of the free-electron model where the jump at the Fermi momentum is unity. If the electron-electron interaction makes the step at the Fermi momentum smaller, the factor will not be $\frac{1}{2}$ but will be greater than $\frac{1}{2}$.

## VI. CONCLUSIONS

We have demonstrated that the $\gamma$-ray angular-correlation curve will have a sharp kink at the Fermi momentum of normal metals, even though the effects of the Coulomb force of the positron cause major changes in the electronic motion, in particular, the annihilation rates. We have also shown a connection of the slope of the angular-correlation curve with the Gaussian curvature of the surface. It is hoped that these will be useful for detailed analysis of the Fermi surfaces by the positron-annihilation techniques.

## ACKNOWLEDGMENTS

The work was carried out at the University of California, La Jolla, and supported by the U. S. Office of Naval Research. I would like to thank Professor W. Kohn for suggesting the problem and for guidance throughout the work. It is a pleasure to acknowledge many discussions with Dr. K. Sawada, Dr. R. Balian, Dr. J. M. Luttinger, and many others at La Jolla.